IEEE Access
Multidisciplinary | Rapid Review | Open Access Journal

Received July 18, 2020, accepted August 5, 2020, date of publication August 17, 2020, date of current version September 25, 2020.

Digital Object Identifier 10.1109/ACCESS.2020.3017280

Path Tracking Control Based on the Prediction of Tire State Stiffness Using the Optimized Steering Sequence

SHAOSONG LI[1], SHUJUN WANG[1], SHUAI WANG[1], NIAONA ZHANG[2], AND GAOJIAN CUI[1]
[1]School of Mechatronic Engineering, Changchun University of Technology, Changchun 130012, China
[2]School of Electrical and Electronic Engineering, Changchun University of Technology, Changchun 130012, China

Corresponding author: Niaona Zhang (zhangniaona@163.com)

This work was supported in part by the National Natural Science Foundation of China under Grant 51905045, and in part by the Key Technology on Major Program of Jilin Province under Grant 20170201005GX.

ABSTRACT This study proposes a linear time-varying model predictive control method based on tire state stiffness prediction for the path tracking using a steering decision sequence in a prediction horizon. A nonlinear UniTire model is employed to represent the nonlinear features of vehicle dynamics in critical situations. And the changing trend of tire state stiffness over the prediction horizon is constructed based on the steering decision sequence, which is the optimized solution of the previous execution step by the controller. Moreover, a method of adjusting the tire state stiffness is proposed to address the jittering in the process of linearization. Meanwhile, a nonlinear model predictive controller and a traditional linear time-varying model predictive controller are designed to verify the effectiveness of the proposed linearization method. Experimental results clearly show that this linearization method can considerably improve vehicle stability under extreme conditions.

INDEX TERMS Path tracking, tire state stiffness, model predictive control, vehicle dynamics.

I. INTRODUCTION

In recent years, with the rapid development of urban roads and transportation technology [1], [2], the number of vehicles has increased dramatically. With the increasing maturity of control technology and the continuous improvement of driver requirements for maneuverability, safety, efficiency and comfort of driving, autonomous vehicles have received attention. To improve road traffic safety, safety technology, which is represented by the advanced driving assistance system (ADAS), has gradually received attention and has been developed [3], [4]. The ADAS detects the environmental information based on on-board sensors and then controls the vehicle through active intervention in emergencies. In recent years, the ADAS has gradually developed from the early anti-lock braking system to the emergency collision avoidance system. The existing emergency avoidance system mainly focuses on the low-speed working condition and only relies on braking to avoid collision with obstacles.

The associate editor coordinating the review of this manuscript and approving it for publication was Razi Iqbal.

However, this method may not be the most effective way to avoid collision in high speed or during emergencies conditions. Compared with collision avoidance system by braking, active steering is an effective way for high-speed avoidance. In the process of high-speed emergency avoidance based on active steering, the reference path is planned by a controller according to the information of the surrounding environment [5], [6]. Then, the vehicle is controlled to track the planned path. Under some extreme conditions, the vehicle may be close to the dynamic limit. Therefore, the driving stability of vehicle in path tracking control can not be ignored. Control methods for path tracking mainly include PID control, sliding mode control, and feedforward-feedback control [7]–[12]. However, these control methods usually consider incomplete kinematic constraint, and ignore the various dynamics of the vehicle during path tracking. Model predictive control (MPC) has the features of prediction, rolling optimization, and feedback correction. It is especially suitable for establishing an accurate controlled object model, dealing with uncertain environmental interference and control systems with constraints [13], [14]. Therefore, MPC

has been widely used in the field of vehicle control. During the process of vehicle control, the accuracy of the model is very important for the stability control [15].

Tires are the largest nonlinear portion in a vehicle system. When the vehicle is in emergency conditions, handling stability is constrained by the high nonlinearity of tires. Thus, establishing a high-precision nonlinear tire model to improve the stability of the vehicle is of great significance. However, the computation complexity caused by using a nonlinear dynamics model is an important reason that hinders its popularization and application. Numerous studies focused on the nonlinearity of tires. Some studies made a small angle approximation of the slip angle of tires and have simplified the vehicle with a linear model [16], [17]. To describe this traditional linear model, we record it as LTI-MPC to distinguish the linear time-varying model in the following. This simplified linear vehicle model performs well when the tire force is in the linear region. However, the accuracy of path tracking and the effect of vehicle stability become worsen at extreme conditions. In this regard, some researchers designed a linear time-varying model predictive controller (LTV-MPC) to improve vehicle performance in a limiting condition. The linear time-varying controller successively linearizes the nonlinear tire model based on the state parameters of the vehicle [18]–[20]. However, when the motion of the vehicle is approaching at the limit conditions of vehicle dynamics, tire force gradually tends to the nonlinear region and becomes inaccurate. Therefore, some researchers proposed the idea of successively linearizing a non-linear vehicle model over the prediction horizon. Katriniok and Abel [21] proposed a linearization method that using an estimated front steering angle for linearization of the nonlinear prediction model. The simulation results show that the control performance of LTV-MPC based on the estimated front wheel angle is improved considerably. Funke *et al.* [22]–[24] proposed a linearization method and the previous tire sideslip angle was utilized for the linearization at the prediction horizon. However, it may cause the system to oscillate that only using the tire slip angle sequence at the previous execution step. To overcome the problem of oscillation, a regularization method [24] is applied to the tire slip angle sequence, which effectively reduces the jittering. However, this method requires that the length of the control horizon is consistent with the length of the prediction horizon, which greatly increase the calculation load and reduce the real-time performance of the controller. Li *et al.* [25] proposed a state stiffness method based on the reference path to improve the stability of the vehicle. The required tire force is obtained by substituting the reference path information into the vehicle model. However, this substitution may increase the complexity of the model.

Therefore, to describe the changing trend of tire force accurately and improve the stability of vehicles over the prediction horizon, this study proposes a linear time-varying model prediction based on the steering decision sequence. The first value of the steering decision is used to control the vehicle, and the rest of the steering decision sequence, which represents the future state of the vehicle in the prediction horizon, is used to forecast the future state stiffness. Then the predicted tire state stiffness is employed to linearize the tire force over the prediction horizon. To verify the effectiveness of the proposed controller, it is compared with a LTI-MPC controller and a nonlinear model predictive controller in the same operating conditions.

Compared with the previous work, the improvements are as follows: 1) In this article, the optimized steering angle sequence is directly used to predict the change trend of tire state stiffness in the prediction horizon. Therefore, the controller model is further simplified. 2) In addition, the prediction of tire state stiffness is divided into two different parts and the changing trend of tire state stiffness is refined. Thus, the stability of the vehicle under extreme condition is effectively improved.

The remainder is structured as follows. Section II presents the vehicle and tire models used by controller. Section III introduces the overall structure of the controller. In Section IV, the experimental and simulation results are presented under different conditions. Finally, conclusions are made in Section V.

II. SYSTEM MODELING

A. VEHICLE MODEL

In this section, a simplified four-wheel bicycle model combined with a nonlinear tire model is used to design the controller. The influence of suspension motion, aerodynamic factors and the longitudinal dynamics are ignored before establishing the model. And the detailed vehicle model is depicted in Fig.1.

Assuming that the steering angle of the vehicle is small and the longitudinal velocity of vehicle is constant, the vehicle dynamics can be expressed as follows:

$$\begin{aligned} &m\dot{x}(\dot{\beta}+r) = F_{yf} + F_{yr} \\ &I_z\dot{r} = \left(aF_{yf} - bF_{yr}\right) \\ &\dot{\varphi} = r \\ &\dot{Y} = \dot{x}\sin\varphi + \dot{y}cos\varphi \end{aligned} \tag{1}$$

where m is the total mass of the vehicle, $\dot{x}$ represents the longitudinal velocity of the vehicle, I_z is the moment of inertia of the vehicle about the z-axis, β is the vehicle sideslip angle, φ is the yaw angle, Y is the lateral position of the vehicle in the geodetic coordinate system, and F_{yf} andF_{yr} represent the lateral force on the front and rear axle of the vehicle, respectively. Moreover, $F_{yf} = F_{y,fl} + F_{y,fr}$ and $F_{yr} = F_{y,r_l} + F_{y,rr}$. The detailed vehicle model parameters are shown in Table 1.

B. TIRE MODEL

Tire force is the main factor that affects vehicle stability, especially when the vehicle is at the limits of dynamic. Therefore, using a high-precision tire model is necessary to describe the change of tire force accurately. Commonly used tire models include the Dugoff tire model, the Magic Formula tire model, the Fiala tire model, and the UniTire model. The UniTire

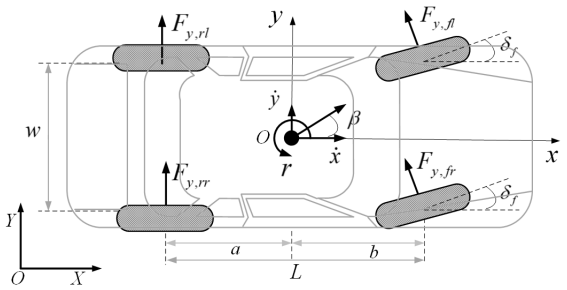

FIGURE 1. Simplified four wheels bicycle model.

TABLE 1. Parameters of vehicle model.

Symbol	Description
m	Vehicle mass
a	Distance from COG to front axle
b	Distance from COG to rear axle
w	Distance between left and right wheels
L	Distance between front and rear axles
δ_f	Steering angle at front axle
$\dot{x}$	Longitudinal velocity of the COG
$\dot{y}$	Lateral velocity of the COG
φ, r	Yaw angle, yaw angle rate
$F_{y,fl}/F_{y,fr}$	Lateral force at left/right front wheel
$F_{y,rl}/F_{y,rr}$	Lateral force at left/right rear wheel

model can describe the tire characteristics of the vehicle in complex conditions with fewer parameters and high accuracy. This study employs a UniTire model according to [26]–[28].

The lateral force of the UniTire model is expressed as follows:

$$F_{yi} = \bar{F}_{yi}\mu_{yi}F_z = m_i\bar{F}_{yi} \tag{2}$$

$$\bar{F}_{yi} = 1 - \exp\left[-\phi_i - E_{1i}\phi^2 - \left(E_{1i}^2 + \frac{1}{12}\right)\phi_i{}^3\right] \tag{3}$$

$$\phi_i = \left|\frac{k_{yi}\tan\alpha_i}{\mu_{yi}F_{zi}}\right| = |n_i\tan\alpha_i| \tag{4}$$

where F_{yi} is the tire lateral force, $\bar{F}_{yi}$ is dimensionless tire cornering force, μ_{yi} is the coefficient of lateral friction; F_{zi} denotes tire vertical load, ϕ_i is the dimensionless lateral slip rate, α_i and denotes the tire side slip angle. The detailed meaning and the value of letters in the formula are shown in our previous study [25] and will not repeated in this study.

III. MODEL PREDICTIVE CONTROLLER DESIGN

A. OVERALL FRAMEWORK OF THE CONTROLLER

Model prediction control is a finite prediction horizon optimization strategy that moves forward through time as shown in Fig.2. This rolling optimization strategy can make up for the uncertainty caused by model mismatch, time-variation and interference. At each time step k, the controller optimizes a set of input sequence by solving an open-loop optimization problem online. This study proposes a LTV-MPC method by making full use of the state information in the prediction horizon.

The ensemble framework of the controller in this study is shown in Fig.3. The framework mainly includes three

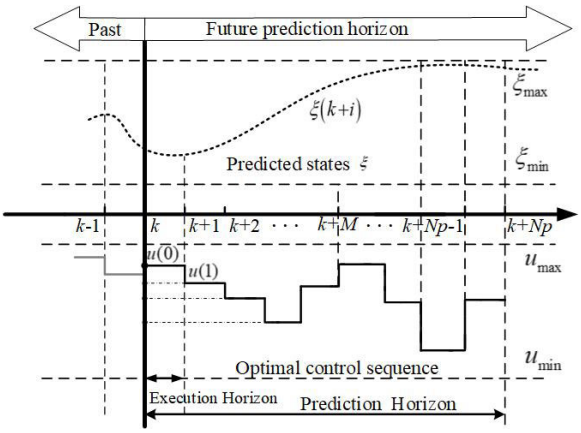

FIGURE 2. Principle of the model prediction scheme.

parts. The MPC controller optimizes the solution according to the reference value and the feedback vehicle states, and obtains the input steering decision sequence. Then, the optimal control input sequence over the current horizon is utilized to predict the tire stiffness for the next prediction horizon. We suppose that the collision avoidance trajectory of the vehicle has been completed by the path planner, which will not be discussed in the remainder of this study. This section designs two different controllers to compare the proposed LTV-MPC method. One is a LTI-MPC controller, and the other is a NMPC controller. Finally, the proposed LTV-MPC is introduced in detail.

B. RESULTING NONLINEAR MPC

The vehicle dynamic described by (1) can be written as follows:

$$\begin{aligned} \dot{\xi}(t) &= f(\xi(t), u(t)) \\ y_c(t) &= C\xi(t) \end{aligned} \tag{5}$$

where

$$\xi = [\beta, r, \varphi, Y]^T \quad u = \delta_f$$
$$C = \begin{bmatrix} 1 & 0 & 0 & 0 \\ 0 & 0 & 0 & 1 \end{bmatrix} \quad y_c = [\beta, Y]^T$$

where ξ and u represent the vehicle state vector and the control input, respectively, y_c is the control output and C is the coefficient matrix of the output.

Discretizing the continuous model at sampling time Ts with a zero-order hold method and the discrete nonlinear vehicle model can be achieved.

According to the fundamental of model prediction control, only the first element of the control input sequence is used to control the vehicle for collision avoidance.

C. DESIGN OF LTI-MPC CONTROLLER

The linearization of the traditional linear time-varying controller remains unchanged in the prediction horizon. In [29], the first-order terms of Taylor expansion are employed to linearize the tire model at each sampling time according to

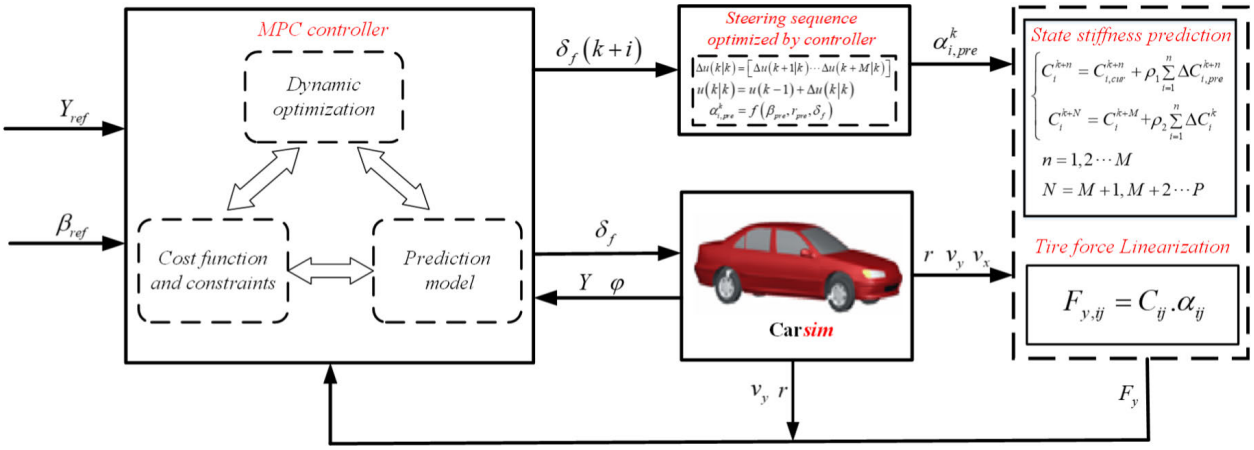

FIGURE 3. The overall structure of controller.

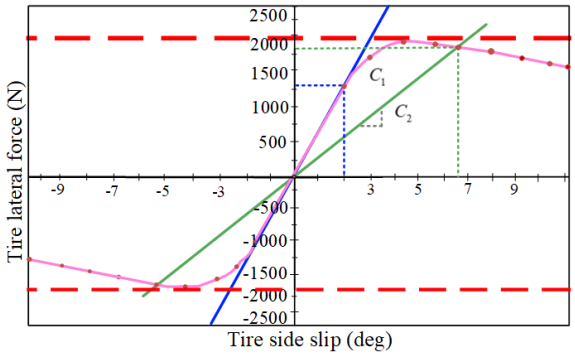

FIGURE 4. Lateral state stiffness.

the current vehicle state. However, this method will introduce the residual lateral force in the process of linearizing, which will lead to the inaccuracy of the model to a certain extent.

The present study employs the state stiffness for linearization. Tire state stiffness was first proposed in [26]. In [25], the tire state stiffness was redefined as shown in Fig.4. It can be expressed as follows:

$$C = F_y^{UniTire}/\alpha \tag{6}$$

Furthermore, the linearization of tire lateral force can be approximated as follows:

$$F_{y,ij}^{UniTire} = C_{ij}.\alpha_{ij} \tag{7}$$

where $ij = [fl, fr, rl, rr]$ represents the four tires of the vehicle, respectively. To improve the calculation speed of (7), a 3D look-up table is employed in this study. And the tire state stiffness can be obtained directly by the 3D look-up table. The front and rear tire slip angle of the vehicle can be simplified as:

$$\alpha_i = f\left(\beta, r, \delta_f\right) \tag{8}$$

Substituting (7) and (8) into (1), the following equation can be obtained:

$$\begin{aligned}
\dot{\beta} &= \frac{C_f + C_r}{m\dot{x}}\beta + \left(\frac{aC_f - bC_r}{m\dot{x}^2} - 1\right)r - \frac{C_f}{m\dot{x}}\delta_f \\
\dot{r} &= \frac{aC_f - bC_r}{I_z}\beta + \frac{a^2C_f + b^2C_r}{I_z\dot{x}}r - \frac{aC_f}{I_z}\delta_f \\
\dot{\varphi} &= r \\
\dot{Y} &= \dot{x}\left(\varphi + \beta\right)
\end{aligned} \tag{9}$$

Choosing δ_f as the control input and $\xi = \left[\beta\ r\ \varphi\ Y\right]^T$ as the vehicle states, the model (9) can be written as follows:

$$\begin{aligned}
\dot{\xi} &= A\xi + B\delta_f \\
y &= C\xi
\end{aligned} \tag{10}$$

where

$$A = \begin{bmatrix} \frac{C_f + C_r}{m\dot{x}} & \frac{aC_f - bC_r}{m\dot{x}^2} - 1 & 0 & 0 \\ \frac{aC_f - bC_r}{I_z} & \frac{a^2C_f + b^2C_r}{I_z\dot{x}} & 0 & 0 \\ 0 & 1 & 0 & 0 \\ \dot{x} & 0 & \dot{x} & 0 \end{bmatrix}$$

$$B = \begin{bmatrix} -\frac{C_f}{m\dot{x}} \\ -\frac{aC_f}{I_z} \\ 0 \\ 0 \end{bmatrix} \qquad C = \begin{bmatrix} 1 & 0 & 0 & 0 \\ 0 & 0 & 0 & 1 \end{bmatrix}$$

where C_f is the lateral stiffness of the front axle, and C_r is the lateral stiffness of the rear axle; Moreover, $C_f = C_{fl} + C_{fr}$ and $C_r = C_{rl} + C_{rr}$.

The continuous model (10) is transformed into an incremental equation as follows:

$$\begin{aligned}
\Delta\xi\left(k+1\right) &= A\Delta\xi\left(k\right) + B_u\Delta u\left(k\right) \\
y_c\left(k\right) &= C\Delta\xi\left(k\right) + y_c\left(k-1\right)
\end{aligned} \tag{11}$$

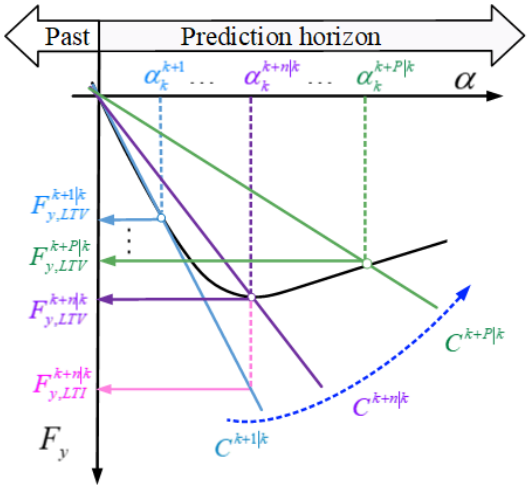

FIGURE 5. Linearization of LTV-MPC.

According to (11), the output of future P steps can be predicted as follows:

$$\xi\left(k+1\,|k\right) = S_\xi \Delta\xi\left(k\right) + I y_c\left(k\right) + S_u \Delta U\left(k\right) \tag{12}$$

where

$$s_\xi = \begin{bmatrix} CA \\ \vdots \\ \sum_{i=1}^{P} CA^i \end{bmatrix}_{P\times 1} \quad I = \begin{bmatrix} I_n \\ \vdots \\ I_n \end{bmatrix}_{P\times 1} \quad I_n = \begin{bmatrix} 1 & 0 \\ 0 & 1 \end{bmatrix}$$

$$S_u = \begin{bmatrix} CB_u & 0 & 0 \\ \vdots & \vdots & \vdots \\ \sum_{i=1}^{P} CA^{i-1}B_u & \cdots & \sum_{i=1}^{P+M-1} CA^{i-1}B_u \end{bmatrix}_{P\times M}$$

D. DESIGN OF THE LTV-MPC CONTROLLER

For LTI-MPC, the state parameters are constantly updated at each sampling time and remain unchanged over the prediction horizon. This method can achieve a satisfactory control effect under normal conditions. However, when the prediction horizon is set to a long time, the LTI-MPC method will produce a considerable error, as illustrated in Fig.5.

In Fig.5, at the step of $k+1$, the tire force is linearized at the slip angle α^{k+1}, which can provide an accurate approximation for the tire force. With the continuous forward movement in the prediction horizon, the linearized tire force produces a huge offset with the actual tire force due to the nonlinear characteristic of the tire. For example, at the step of $k+n$, the tire force $F_{y,LTI}^{k+n}$, obtained by LTI-MPC, has been seriously inconsistent with the actual value.

To solve the above problem, the tire state stiffness for P-step in the future should be predicted accurately. The detailed linearization based on tire state stiffness in the prediction horizon is illustrated in Fig.5.

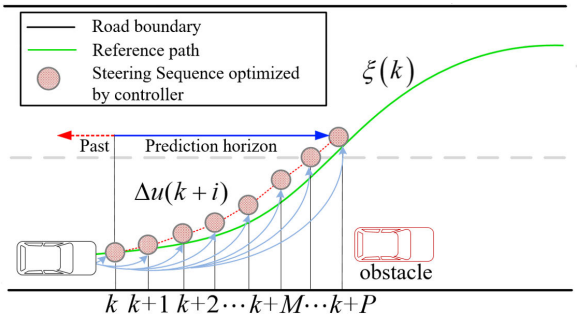

FIGURE 6. Steering decision sequence over prediction horizon.

A series of steering angle sequences are determined by solving an optimal problem that satisfies the objective and constraints over a control time horizon at each time step. The steering decision increment sequence of M step in the control horizon can be obtained as $\Delta u\left(k|\,k\right) = \left[\Delta u\left(k+1|\,k\right)\ \cdots \Delta u\left(k+M|\,k\right)\right]$. The steering decision sequence at time k over the prediction horizon is shown in Fig.6.

At time k, the controller obtains a set of control inputs sequence $u(k+i\,|k)$ and vehicle states $\xi(k+i\,|k)$ in the prediction horizon. The vehicle states in the predicted horizon can be converted into the tire slip angle by (8). For the sake of convenience, we record the predicted tire slip angle over the prediction horizon as $\alpha_{i,pre}^{k}$. Then, the predicted tire slip angle can be expressed as follows:

$$\alpha_{i,pre}^{k} = f\left(\beta_{pre}, r_{pre}, \delta_f\right) \tag{13}$$

where the subscript pre denotes the predicted value and $i = r, l$. β_{pre} and r_{pre} are the predicted vehicle side slip and yaw rate, respectively.

After obtaining the predicted tire slip angle, the tire state stiffness can be predicted by the designed 3D look-up table and can be recorded as $C_{i,pre}^{k+n}$ at time k. Moreover, the incremental form of tire state stiffness can be obtained as follows:

$$\Delta C_{i,pre}^{k+n} = C_{i,pre}^{k+n} - C_{i,pre}^{k+n-1} \tag{14}$$

where $n = 1, 2\cdots M$. According to the basic principle of model prediction, only the first element of the optimized sequence at each sampling time acts on the vehicle. The remaining elements in the current prediction horizon will be used to predict the changing trend of tire state stiffness.

The tire state stiffness at current sampling time is introduced to reduce the deviation of the predicted state stiffness determined by (14). The final predicted state stiffness sequence is as follows:

$$C_i^{k+n} = C_{i,cur}^{k+n} + \sum_{i=1}^{n} \Delta C_{i,pre}^{k+n} \tag{15}$$

where $C_{i,cur}^{k+n}$ is tire state stiffness at the current tire slip angle, which is determined by the 3D look-up table of tire state stiffness.

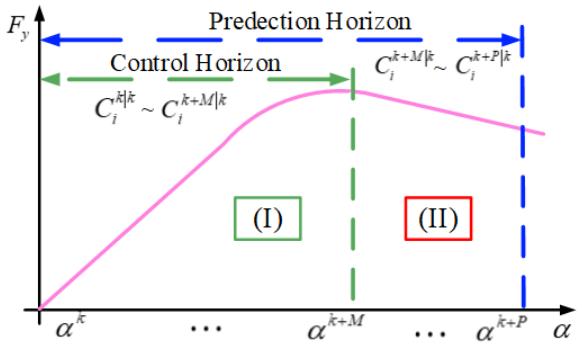

FIGURE 7. Tire State stiffness over prediction horizon.

As shown above, the linearization over the prediction horizon depends on the optimized control input sequence at the previous time. This linearization method requires that the length of the control horizon M is same as that of the predicted horizon P. However, long control horizon will increase the computational burden of the system. Therefore, the length of the control horizon should be shorter than prediction horizon.

In this study, the tire state stiffness from $k+1$ to $k+P$ is employed during the process of model linearization based on the proposed method. Therefore, the predicted state stiffness over the prediction horizon can be divided into two parts as shown in Fig.7.

Region (I) represents the predicted tire state stiffness in the control horizon. In this region, the tire state stiffness $C_i^k - C_i^{k+M}$ entirely depends on the optimized steering angle sequence. The tire state stiffness can be obtained from (14) and (15). Region (II) is the tire state stiffness that ranges from $k+M+1$ to $k+P$. To better improve the prediction accuracy, the following two prediction methods are designed.

1) TIRE STATE STIFFNESS REMAINS UNCHANGED FROM *M* TO *P*

When MPC is used to predict the future states of the system, the control variables outside the control horizon are usually assumed to remain unchanged, that is, $\Delta u(k+i) = 0,\ i = M, M+1 \cdots P-1$. Therefore, the tire state stiffness outside the control horizon remains unchanged too. The future tire state stiffness is expressed follows:

$$\begin{cases} C_i^{k+n} = C_{i,cur}^{k+n} + \sum_{i=1}^{n} \Delta C_{i,pre}^{k+n} & n = 1, 2 \cdots M \\ C_i^{k+n} = C_i^{k+M} & n = M+1, M+2 \cdots P \end{cases} \tag{16}$$

where C_i^{k+M} is the predicted tire state stiffness at step M. Once the changing trend of the tire state stiffness is determined, tire force can be linearized according to (7). For convenience, we record this linearization as LTV*-MPC.

2) TIRE STATE STIFFNESS FROM *M* TO *P* IS VARIABLE

When the vehicle is in an emergency condition, the above tire state stiffness prediction method may not be accurate. This section proposes a weighting adjustment method for tire state stiffness to improve the accuracy of prediction. And the increment of tire state stiffness is introduced as follows:

$$\Delta C_i^k = C_i^k - C_{i,prev}^{k-1} \tag{17}$$

where C_i^k is the tire state stiffness at the current tire slip angle, $C_{i,prev}^{k-1}$ indicates the tire state stiffness of the previous time and ΔC_i^k is the increment between the state stiffness at the current time and the last time.

Finally, the tire state stiffness ranging from $k+M+1$ to $k+P$ relies on ΔC_i^k. And this linearization method is recorded as LTV-MPC. The changing trend can be expressed as follows:

$$\begin{cases} C_i^{k+n} = C_{i,cur}^{k+n} + \rho_1 \sum_{i=1}^{n} \Delta C_{i,pre}^{k+n} & n = 1, 2 \cdots M \\ C_i^{k+n} = C_i^{k+M} + \rho_2 \sum_{i=1}^{n} \Delta C_i^k & n = M+1, M+2 \cdots P \end{cases} \tag{18}$$

where ρ_1 and ρ_2 are the weighting factors of state stiffness.

Substituting (17) and (18) into (7), the linearization of the tire force over the predicted horizon is as follows:

$$F_{y,i}^{k+n} = C_i^{k+n} . \alpha_i^{k+n} \tag{19}$$

The linearized tire force in (19) is further substituted into (9). Then the LTV-MPC prediction model can be expressed as follows:

$$\begin{aligned} \Delta\xi(k+1) &= A_t^k \Delta\xi(k) + B_t^k \Delta u(k) \\ y_c(k) &= C\Delta\xi(k) + y_c(k-1) \end{aligned} \tag{20}$$

where A_t^k and B_t^k are the coefficient matrix.

E. COST FUNCTION OF CONTROLLER

In order to track the predefined path well, the deviation between the actual trajectory and the reference value should be as small as possible. And the vehicle sideslip angle should also be as small as possible to guarantee the stability of vehicle. In addition, steering smoothness should be guaranteed. Finally, the cost function can be written as follows:

$$\begin{aligned} \textit{minimize} \quad & \sum_{n=1}^{P} \left[\left(Y(k+n) - Y_{ref}(k+n) \right)^2 \cdot \Gamma_y \right] \\ & + \sum_{n=1}^{P} \left[\left(\beta(k+n) - \beta_{ref}(k+n) \right)^2 \cdot \Gamma_\beta \right] \\ & + \sum_{n=1}^{M} \left[\left(\Delta\delta_f (k+n-1)^2 \right) \cdot \Gamma_u \right] \end{aligned} \tag{21}$$

$$\begin{aligned} \textit{subject to} \quad & -u_{\max} \le u(k+n) \le u_{\max} \\ & -\Delta u_{\max} \le \Delta u(k+n) \le \Delta u_{\max} \\ & n = 0, 1 \cdots M \end{aligned} \tag{22}$$

where Γ_y is the weighting matrix of lateral displacement, and Γ_β and Γ_u is the weighting matrix of vehicle sideslip and control input δ_f, respectively.

Therefore, the optimization problem can be transformed into a constrained QP problem as follows:

$$\min_z z^T H z - g^T z \quad \bar{C} z < \bar{b} \tag{23}$$

where $z = \Delta u(k)$ is the independent variables of the optimization problem, H denotes the Hessian matrix, g represents the gradient vector. $\bar{C}$ and $\bar{b}$ are the constraints. These detailed expressions are as follows:

$$\begin{aligned} H &= 2\left(S_u^T \Gamma_y^T \Gamma_y S_u + \Gamma_u \Gamma_u\right) \\ g &= -2 S_u^T \Gamma_y^T \Gamma_y E_P \\ E_P &= R(k+1) - S_\xi \Delta x(k) - I \cdot y_c(k) \\ \bar{C} &= [I^T, -I^T, L^T, -L^T]^T_{4M\times 1} \\ \bar{b} &= \begin{bmatrix} \Delta U(k)_{\max} \\ -\Delta U(k)_{\min} \\ U_{\max}(k) - u(k-1) \times ones(M,1) \\ u(k-1) \times ones(M,1) - U_{\min}(k) \end{bmatrix}_{4M\times 1} \end{aligned}$$

For NMPC, the fmincon programming algorithm of the MATLAB tool is employed to solve the optimization problem. After a set of optimal control sequences are obtained, only the first element of the sequence is applied to the system.

IV. SIMULATION RESULTS

To test the performance of the proposed method, numerical simulations are performed based on MATLAB and CarSim environments. These simulation experiments mainly include two parts. Firstly, the accuracy of the predicted tire state stiffness is verified. And then the path tracking effect of the three kinds of controllers are verified under different conditions. In the previous work [25], the accuracy of the UniTire model was verified, and the results show that the UniTire model has a high precision, which will not be discussed again in this study.

A. VERIFICATION OF PREDICTED TIRE STATE STIFFNESS

To verify the accuracy of the proposed state stiffness prediction method, we compare the predicted state stiffness with the actual state stiffness. The vehicle speed is 80km/h and the tire-road friction coefficient is 0.3.

The state stiffness of the front and rear tire are shown in Figs. 8 and 9, respectively. C_{real} denotes the actual value of tire state stiffness. In this article, a 3D Look-up table of tire state stiffness according to tire slip angle and vertical load is designed based on UniTire model. And the actual tire slip angle and vertical load are exported from Carsim. Finally, the actual tire slip angle and vertical load are inputted into the 3D Look-up table to obtain the actual tire state stiffness. The predicted C_{pre}^1 and C_{pre}^2 are the first and second value of the predicted tire state stiffness sequence over the prediction horizon. The peak of predicted tire state stiffness is revealed to deviates slightly from the actual state stiffness value at 3.8 s and 4.65 s. In Fig. 8, the maximum deviation of front tire state stiffness occurs in 4.36 s, and the maximum deviation value is approximately 9985 N/rad. Fig. 9 shows the predicted tire state stiffness curve of the rear tires. The rear tire state stiffness achieves the peak near 3.9 s,and the maximum deviation value of 6692 N/rad occurs at 4.36 s. The results show that there is a certain deviation between the predicted tire state stiffness and the actual value at the peak. However, the overall changing trend of the predicted tire state stiffness is basically consistent with that of the actual tire stiffness. This verification indicates that the predicted tire state stiffness can ensure the accuracy of linearization.

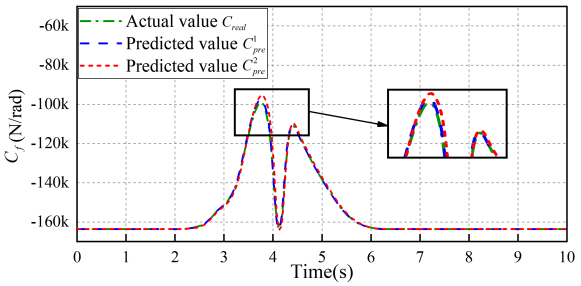

FIGURE 8. State stiffness of front tires.

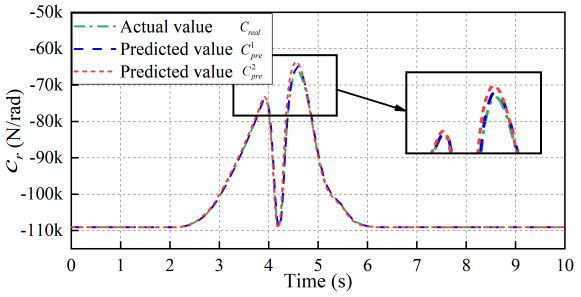

FIGURE 9. State stiffness of rear tires.

B. PATH TRACKING TEST

In this section, the effectiveness of the proposed linear time-varying controller is evaluated by comparing with the designed LTI-MPC and NMPC controllers. The experiment is simulated under a scene of lane change maneuver of vehicle at different speeds and road conditions. And the trajectory of lane change maneuver is shown in Fig. 10. In addition, the main parameters of vehicle and controllers are shown in Table 2.

1) LANE CHANGE TEST FOR LTV*-MPC

The experiment is simulated at a speed of 80km/h and the tire-road coefficient is 0.3. Figs. 11(a)-11(d) are the state curves of the controllers. The trajectory curve of the vehicle is shown in Fig. 11(a). It can be seen that three kinds of controllers can control the vehicle to track reference trajectory well.

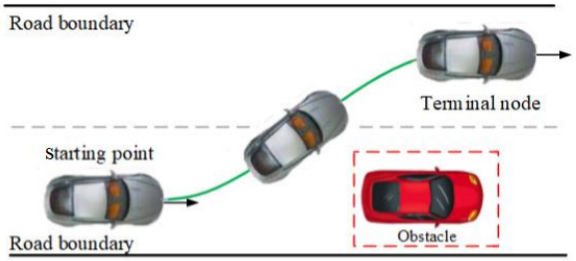

FIGURE 10. Lane change trajectory.

TABLE 2. Simulation parameters.

vehicle parameters	Symbol	Value	Units
Distance from COG to front axle	a	1.04	m
Distance from COG to rear axle	b	1.56	m
Distance between the left and right wheels	w	1.481	m
Yaw moment of inertia	I_z	2031.4	kg·m^2
Vehicle mass	m	1240	kg
Controller parameters	**LTI-MPC**	**LTV-MPC**	**NMPC**
Discrete time	0.01	0.01	0.01
Prediction horizon	50	50	50
Prediction horizon	5	50	1
Weighting factor ρ_1	0	1.6	$none$
Weighting factor ρ_2	0	1.588	$none$

However, the lateral position of the NMPC vehicle has a slight deviation compared with that of the LTI-MPC and LTV*-MPC at X = 110 m. From Fig. 11(b), it can be seen that the peak value of the yaw angle of NMPC is the smallest. In addition, the changing trend of LTV*-MPC and LTI-MPC are basically consistent.

The front steering angle is illustrated in Fig. 11(c). It can be seen that the vehicle starts turning at 2 s and completes the lane changing at 6.5 s. The front steering angle of NMPC is more smooth and achieves the maximum value of 1.6° at 3.4 s and the minimum value of −1.6° at 4.6 s, respectively. With regard to LTI-MPC, the maximum front steering angle value 1.8° is achieved at 3.5 s and the minimum value of −1.8° is achieved at 4.2 s. In addition, the front steering angle of LTI-MPC fluctuates considerably at 4.5 s and jitters continuously after 5 s. Compared with LTI-MPC, LTV*-MPC becomes smooth after a slight fluctuation.

Fig. 11(d) demonstrates the vehicle side slip angle. The maximum and minimum of vehicle side slip angle for LTV*-MPC and LTI-MPC controllers are 0.61°, −0.32° and 0.55°, −0.3°, respectively. The vehicle side slip angle obtained by the designed three kinds of controllers are all within the constraints, which represent the good stability of the controllers under this condition.

To further verify the performance of the controller under limit conditions, experiment is tested at a speed of 100 km/h and the tire-road friction coefficient is 0.4.

Figs.12(a) and (b) show that the vehicle controlled by LTI-MPC controller begins to lose path tracking ability at X = 110 m and completely loses it after X = 150 m. And the

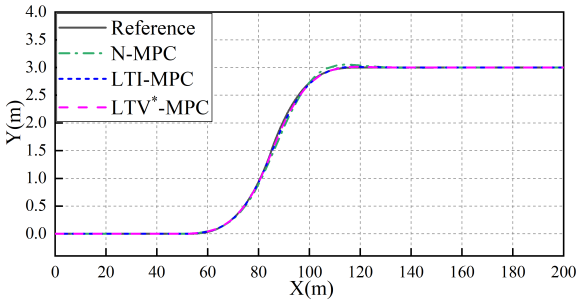

(a) Lateral displacement of tracking.

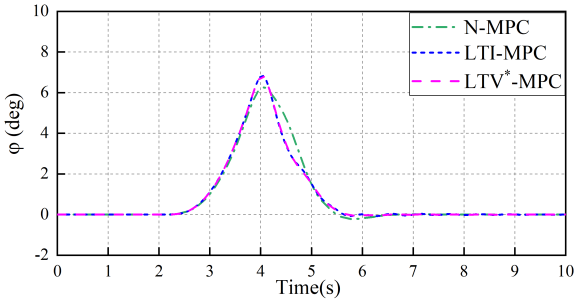

(b) Yaw angle of vehicle.

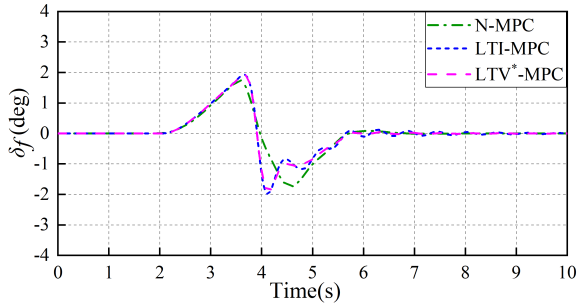

(c) Front steering angle of the vehicle.

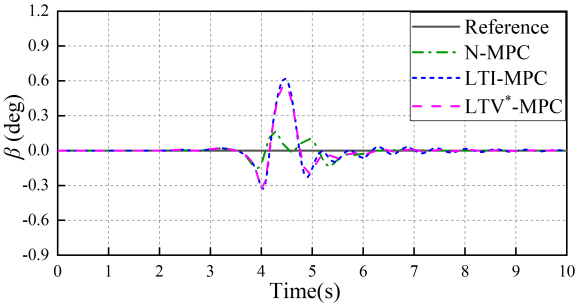

(d) Vehicle sideslip angle.

FIGURE 11. Vehicle state curves at 80km/h.

yaw of the vehicle in Fig. 12(b) exceeds the constraint value. This is caused by the fluctuation of the front steering angle. As shown in Fig. 12(c), the fluctuating of the front steering angle is obvious from 4 s to 5.5 s, even reaching the limit value 10°. And then it decreases rapidly from the maximum value to the minimum value from 5.8 s to 7 s. Compared with LTI-MPC, LTV*-MPC can basically complete the path tracking. However, the front steering angle of LTV*-MPC still has obvious oscillation as shown in Fig. 12(c).

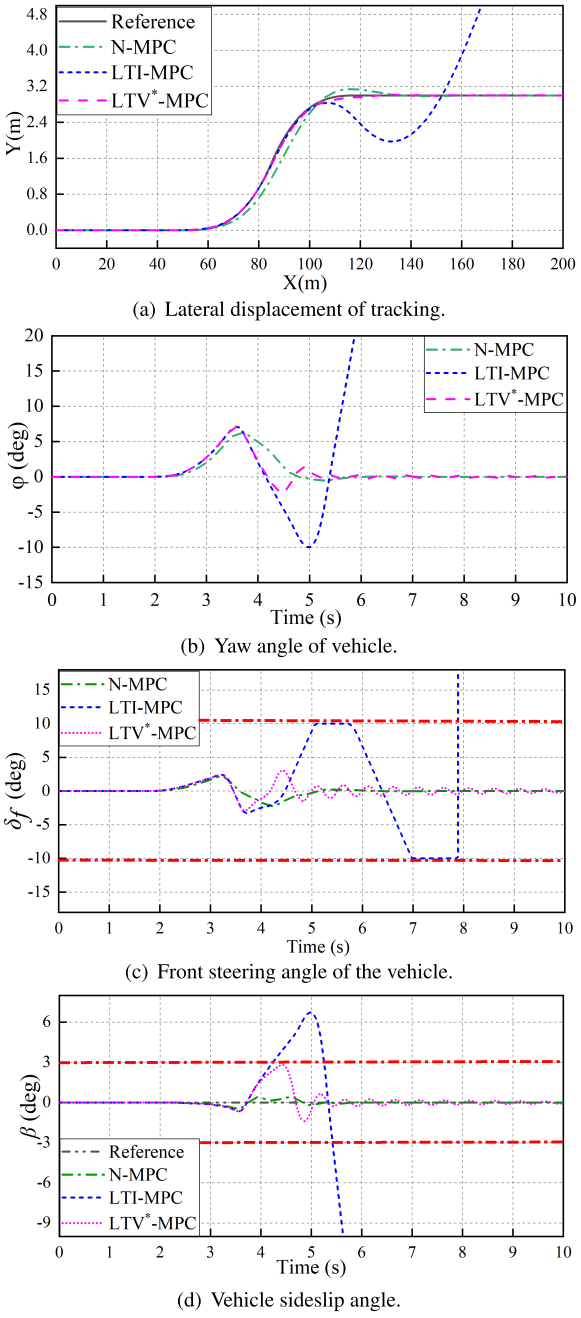

(a) Lateral displacement of tracking.

(b) Yaw angle of vehicle.

(c) Front steering angle of the vehicle.

(d) Vehicle sideslip angle.

FIGURE 12. Vehicle state curves at 100km/h.

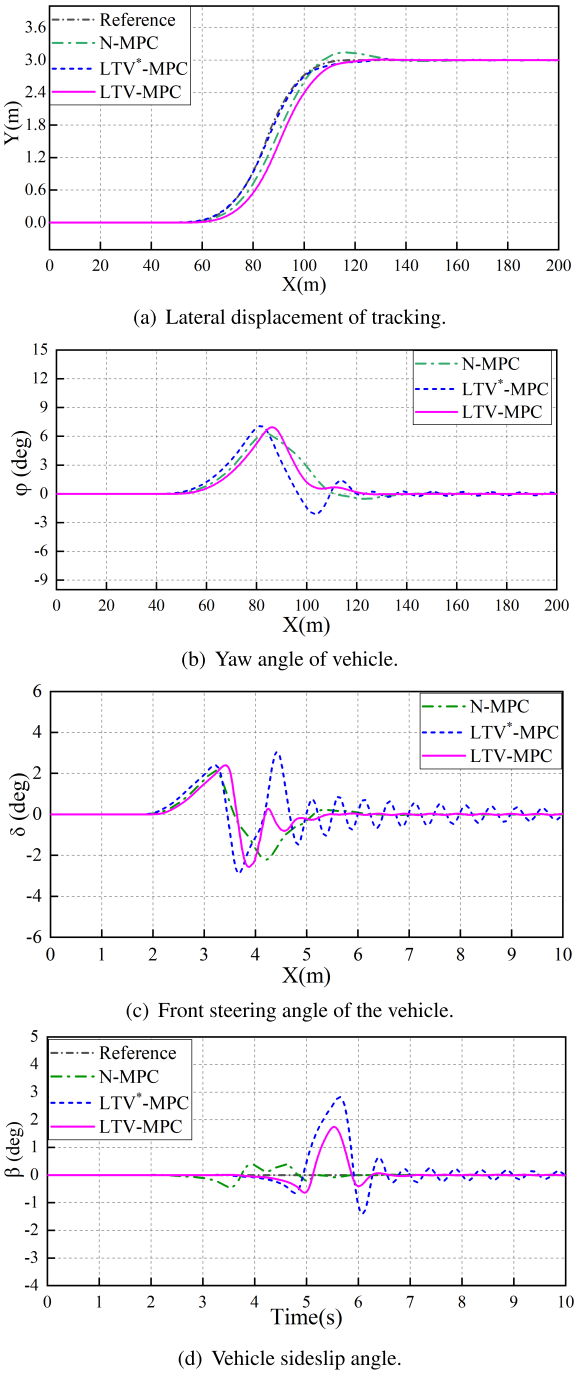

(a) Lateral displacement of tracking.

(b) Yaw angle of vehicle.

(c) Front steering angle of the vehicle.

(d) Vehicle sideslip angle.

FIGURE 13. Vehicle state curves at 100km/h of LTV-MPC.

The vehicle side slip angle of LTI-MPC in Fig. 12(d) become enormous at 4.8 s, which is caused by the excessive front steering angle shown in Fig. 12(c). For LTV*-MPC, the maximum value of vehicle side slip angle is 2.7° at 4.5 s, which is almost three times as much as that of NMPC. Overall, vehicle controlled by LTV*-MPC controller can track the reference trajectory. However, it cannot guarantee the good vehicle stability during path tracking.

2) LANE CHANGE TEST FOR LTV-MPC

In this section, the performance of the proposed LTV-MPC controller is verified. In the above test, the front steering angle of LTV*-MPC has a serious jittering under the speed of 100km/h and the tire-road friction coefficient of 0.4. Given that LTV-MPC is designed based on LTV*-MPC, this linearization method is verified under the same condition.

Figs.13(a) and (b) show that the proposed LTV-MPC can track the reference trajectory well. The yaw angle of LTV-MPC is the smoothest compared with LTI-MPC and LTV*-MPC controllers. Both the yaw angle of NMPC and LTV-MPC has a slight fluctuation near X = 115m. However,

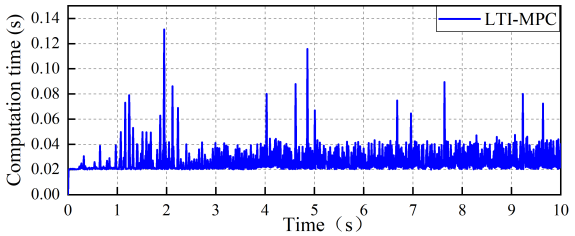

FIGURE 14. Computation time of LTI-MPC.

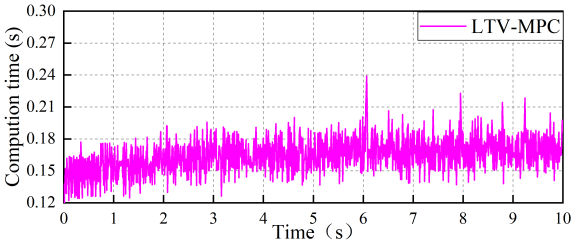

FIGURE 15. Computation time of LTV-MPC.

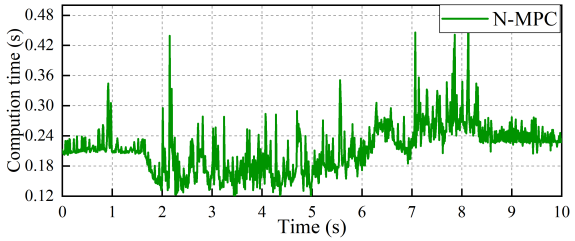

FIGURE 16. Computation time of NMPC.

for LTV-MPC*, the range of the yaw angle fluctuation is enlarged near to −2°. This fluctuation is caused by the fluctuation of the front steering angle optimized by the LTV*-MPC controller form 3.5 s to 5 s, as shown in Fig. 13(c).

Fig. 13(d) shows that the peak of the vehicle side slip angle controlled by LTV*-MPC controller is the largest and that of LTV-MPC is considerably decreased compared with LTV*-MPC. This represents that the proposed LTV-MPC method can effectively improve the stability of the vehicle under limit conditions. Meanwhile, the LTV-MPC method can effectively eliminate the oscillation. However, the maximum value of vehicle side slip angle controlled by LTV-MPC controller is about 1.6°, which is bigger than that of NMPC controller. This is due to the reason that the control horizon length of LTV-MPC controller is 5, while that of NMPC is 1.

Remark: In this article, the length of control horizon is determined by repeated debugging to ensure the best control effect of the controllers. Thus, the length of control horizon of linear controller is not same as nonlinear controller.

Figs. (14)-(16) show the calculation time of LTI-MPC, LTV-MPC and NMPC controllers. The simulation test is carried out on a personal computer, and the computer configuration is as follows: CPU: Intel (R) Core (TM) i5-8250U @ 1.60GHz; RAM: 4.00 GB. It can be seen that the calculation time of NMPC controller is the largest and that of LTI-MPC controller is the smallest. The average computing time of the NMPC is 1.5 times of LTV-MPC. The results of the computation time show that LTV-MPC has faster computation speed than nonlinear MPC, but need to be further improved compared with LTI-MPC.

V. CONCLUSION

In this study, a path tracking control method based on the prediction of tire state stiffness is proposed. This method utilizes the optimized front steering angle sequence to predict the tire state stiffness. And then the predicted tire state stiffness is used to linearize the vehicle model in prediction horizon. The path tracking capability are validated under different working conditions. The results show that the proposed method has good performance in path tracking and can effectively improve the stability of the vehicle.

In this article, the length of prediction horizon is determined by repeated debugging. However, under limit conditions, the stability of the system may be affected by the length of the prediction horizon. In the future work, we will try to design an adaptive predictive horizon controller to improve the stability of path tracking. In addition, we will study the collision avoidance control combined with steering and braking system. And the performance of the controller considering gradually change of speed, mass transfer while accelerating and decelerating will also be considered.

REFERENCES

[1] S. E. Li and H. Peng, "Strategies to minimize the fuel consumption of passenger cars during car-following scenarios," *Proc. Inst. Mech. Eng. D J. Automobile Eng.*, vol. 226, no. 3, pp. 2107–2112, 2011.

[2] F.-Y. Wang, N.-N. Zheng, D. Cao, C. M. Martinez, L. Li, and T. Liu, "Parallel driving in CPSS: A unified approach for transport automation and vehicle intelligence," *IEEE/CAA J. Automatica Sinica*, vol. 4, no. 4, pp. 577–587, 2017.

[3] U. Ozgüner, T. Acarman, K. A. Redmill, and I. Ebrary, *Autonomous Ground Vehicles*. Norwood, MA, USA: Artech House, 2011.

[4] W. Whyte, *Handbook of Intelligent Vehicles*. London, U.K.: Springer, 2012.

[5] S. Li, Z. Li, Z. Yu, B. Zhang, and N. Zhang, "Dynamic trajectory planning and tracking for autonomous vehicle with obstacle avoidance based on model predictive control," *IEEE Access*, vol. 7, pp. 132074–132086, 2019.

[6] M. Hassanzadeh, M. Lidberg, M. Keshavarz, and L. Bjelkeflo, "Path and speed control of a heavy vehicle for collision avoidance manoeuvres," in *Proc. IEEE Intell. Veh. Symp.*, Jun. 2012, pp. 129–134.

[7] Y. H. Eng, H. Andersen, S. D. Pendleton, M. H. Ang, and D. Rus, "Realizing robust control of autonomous vehicles," in *Proc. Int. Symp. Exp. Robot.*, 2017, pp. 374–386.

[8] M. H. A. Majid and M. R. Arshad, "A fuzzy self-adaptive PID tracking control of autonomous surface vehicle," in *Proc. IEEE Int. Conf. Control Syst., Comput. Eng. (ICCSCE)*, Nov. 2015, pp. 458–463.

[9] P. Sarhadi, A. R. Noei, and A. Khosravi, "Model reference adaptive PID control with anti-windup compensator for an autonomous underwater vehicle," *Robot. Auto. Syst.*, vol. 83, pp. 87–93, Sep. 2016.

[10] B. Mashadi, P. Ahmadizadeh, M. Majidi, and M. Mahmoodi-Kaleybar, "Integrated robust controller for vehicle path following," *Multibody Syst. Dyn.*, vol. 33, no. 2, pp. 207–228, Feb. 2015.

[11] J. X. Xu, Y. J. Pan, and T. H. Lee, "A gain scheduled sliding mode control scheme using filtering techniques with applications to multilink robotic manipulators," in *Proc. Amer. Control Conf.*, 2000, pp. 641–649.

[12] R. A. Cordeiro, J. R. Azinheira, E. C. de Paiva, and S. S. Bueno, "Dynamic modeling and bio-inspired LQR approach for off-road robotic vehicle path tracking," in *Proc. 16th Int. Conf. Adv. Robot. (ICAR)*, Nov. 2013, pp. 1–6.

[13] J. Funke, P. Theodosis, R. Hindiyeh, G. Stanek, K. Kritatakirana, C. Gerdes, D. Langer, M. Hernandez, B. Muller-Bessler, and B. Huhnke, "Up to the limits: Autonomous audi TTS," in *Proc. IEEE Intell. Vehicles Symp.*, Jun. 2012, pp. 541–547.
[14] M. Brown, J. Funke, S. Erlien, and J. C. Gerdes, "Safe driving envelopes for path tracking in autonomous vehicles," *Control Eng. Pract.*, vol. 61, pp. 307–316, Apr. 2017.
[15] R. T. O'Brien, P. A. Iglesias, and T. J. Urban, "Vehicle lateral control for automated highway systems," *IEEE Trans. Control Syst. Technol.*, vol. 4, no. 3, pp. 266–273, May 1996.
[16] G. V. Raffo, G. K. Gomes, J. E. Normey-Rico, C. R. Kelber, and L. B. Becker, "A predictive controller for autonomous vehicle path tracking," *IEEE Trans. Intell. Transp. Syst.*, vol. 10, no. 1, pp. 92–102, Mar. 2009.
[17] F. Borrelli, P. Falcone, T. Keviczky, J. Asgari, and D. Hrovat, "MPC-based approach to active steering for autonomous vehicle systems," *Int. J. Veh. Auto. Syst.*, vol. 3, nos. 2–4, pp. 265–291, 2005.
[18] P. Falcone, F. Borrelli, J. Asgari, H. E. Tseng, and D. Hrovat, "A model predictive control approach for combined braking and steering in autonomous vehicles," in *Proc. Medit. Conf. Control Autom.*, Jun. 2007, pp. 1–6.
[19] P. Falcone, M. Tufo, F. Borrelli, J. Asgari, and H. E. Tseng, "A linear time varying model predictive control approach to the integrated vehicle dynamics control problem in autonomous systems," in *Proc. 46th IEEE Conf. Decision Control*, 2007, pp. 2980–2985.
[20] S. Velhal and S. Thomas, "Improved LTVMPC design for steering control of autonomous vehicle," *J. Phys., Conf. Ser.*, vol. 783, 2017, Art. no. 012028.
[21] A. Katriniok and D. Abel, "LTV-MPC approach for lateral vehicle guidance by front steering at the limits of vehicle dynamics," in *Proc. IEEE Conf. Decision Control Eur. Control Conf.*, Dec. 2011, pp. 1–8.
[22] J. Funke, M. Brown, S. M. Erlien, and J. C. Gerdes, "Collision avoidance and stabilization for autonomous vehicles in emergency scenarios," *IEEE Trans. Control Syst. Technol.*, vol. PP, no. 99, pp. 1204–1216, Jul. 2016.
[23] C. E. Beal and J. C. Gerdes, "Model predictive control for vehicle stabilization at the limits of handling," *IEEE Trans. Control Syst. Technol.*, vol. 21, no. 4, pp. 1258–1269, Jul. 2013.
[24] J. Funke, M. Brown, S. M. Erlien, and J. C. Gerdes, "Prioritizing collision avoidance and vehicle stabilization for autonomous vehicles," in *Proc. IEEE Intell. Vehicles Symp. (IV)*, Jun. 2015, pp. 1134–1139.
[25] S. Li, G. Wang, G. Chen, H. Chen, and B. Zhang, "Tire state stiffness prediction for improving path tracking control during emergency collision avoidance," *IEEE Access*, vol. 7, pp. 179658–179669, 2019.
[26] N. Xu, K. Guo, and X. Zhang, "UniTire model for tire forces and moments under combined slip conditions with anisotropic tire slip stiffness," *SAE Int. J. Commercial Vehicles*, vol. 6, no. 2, pp. 315–324, Sep. 2013.
[27] K. Guo, "Unitire: Unified tire model," *J. Mech. Eng.*, vol. 52, no. 12, pp. 90–99, 2016.
[28] K. Guo and D. Lu, "UniTire: Unified tire model for vehicle dynamic simulation," *Vehicle Syst. Dyn.*, vol. 45, no. 1, pp. 79–99, Jan. 2007.
[29] M. Choi and S. B. Choi, "MPC for vehicle lateral stability via differential braking and active front steering considering practical aspects," *Proc. Inst. Mech. Eng. D J. Automobile Eng.*, vol. 230, no. 40, pp. 459–469, 2015.

SHAOSONG LI received the Ph.D. degree in automotive engineering from Jilin University, Jilin, China.

While at Jilin University, he focused on vehicle dynamics and control. He is currently the Director of Vehicle Engineering Department, Changchun University of Technology. His current research interests include the application of control systems to vehicle dynamics to improve safety, stability, and performance of vehicles in conjunction with human drivers. He is a member of the Society of Automotive Engineers of China.

SHUJUN WANG received the bachelor's degree in automotive engineering services from the Henan Institute of Science and Technology, Henan, China. He is currently pursuing the master's degree in automotive engineering with the Changchun University of Technology, Jilin, China.

His research interest includes the theory and technology of automotive safety and model predictive control.

SHUAI WANG received the bachelor's degree in vehicle engineering from Hebei Engineering University, Hebei, China. She is currently pursuing the master's degree in automotive engineering with the Changchun University of Technology, Jilin, China.

Her research interest includes the theory and technology of automotive safety and model predictive control.

NIAONA ZHANG received the Ph.D. degree.

She is currently a Professor with the School of Electrical and Electronic Engineering, Changchun University of Technology. She is also the Head of the RD and Innovation Team for Key Technologies of Electric Vehicle and Chassis Control, Jilin, and the Director of the Engineering Research Center for Complex Electromechanical Equipment Technology, Jilin. Her research interests are the electric vehicle drive theory and control technology, complex system modeling, optimization, and control. She has published two academic monographs, and more than 50 articles on academic journals and international academic conferences. And eight of her published patents were authorized. She carried out and accomplished 16 provincial and municipal scientific research programs, and achieved six provincial and ministerial awards for scientific and technological progress as the first accomplisher.

GAOJIAN CUI received the Ph.D. degree in mechanical design and theory from the Changchun University of Science and Technology, Jilin, China.

He is currently the Vice President of the Automotive Engineering Research Institute, Changchun University of Technology. His current research interests include model-based vehicle dynamics control and intelligent vehicle path planning and tracking.

He was a recipient of the Key Technology on Major Program of Jilin Province.